Effect of vehicle flexibility on the vibratory response of bridge

R. Lalthlamuana and Sudip Talukdar[*]

Department of Civil Engineering, Indian Institute of Technology Guwahati, Guwahati-781039, India

Abstract. In the recent times, dimensions of heavy load carrying vehicle have changed significantly incorporating structural flexibility in vehicle body. The present paper outlines a procedure for the estimation of bridge response statistics considering structural bending modes of the vehicle. Bridge deck roughness has been considered to be non homogeneous random process in space. Influence of pre cambering of bridge surface and settlement of approach slab on the dynamic behavior of the bridge has been studied. A parametric study considering vehicle axle spacing, mass, speed, vehicle flexibility, deck unevenness and eccentricity of vehicle path have been conducted. Dynamic amplification factor (DAF) of the bridge response has been obtained for several of combination of bridge-vehicle parameters. The present study reveals that flexible modes of vehicle can reduce dynamic response of the bridge to the extent of 30-37% of that caused by rigid vehicle model. However, sudden change in the bridge surface profile leads to significant amount of increment in the bridge dynamic response even if flexible bending modes remain active. The eccentricity of vehicle path and flexural/torsional rigidity ratios plays a significant role in dynamic amplification of bridge response.

Keywords: flexibility; deck roughness; non homogeneous; dynamic amplification factor; flexural/torsional rigidity

1. Introduction

The dynamic effect resulting from the passage of vehicles is an important problem generally encountered in the bridge design. The irregularity or unevenness of the bridge pavement surface is the main cause of exciting the vehicle which in turn imposes a time varying load as it travels along the span of the bridge. Starting from the year 1922, various theoretical and experimental studies have been conducted to understand the dynamic behavior of bridge subjected to moving load. A review of literatures on the said topic starting from basic formulation with moving mass has been published by Fryba (1968) and Yang *et al*. (2004) in their books with detail discussion on the formulation and their limitations. Earlier researchers have considered either vehicle as moving load on a bridge by neglecting inertia effect or moving mass incorporating the inertia effect. Although researchers have revealed various dynamic characteristics for practical applications, modern bridges of slender cross section and larger span do not actually reflect true behavior when moving mass problems have been solved. The deformation of bridge can cause significant change in dynamic forces at the contact point of the vehicle wheel. Realizing these facts, numerous studies

---

∗Corresponding author, Professor, E-mail: staluk@iitg.ernet.in

have been conducted considering bridge-vehicle a coupled system, with consideration of stiffness and damping parameters of suspension systems. Wen (1960), Biggs (1964), Fryba (1996) and are some of the authors who considered vehicle as single lumped mass system having only bounce motion or a rigid system with bounce and pitch motion. A three dimensional heave-pitch-roll model has been investigated by Yadav and Upadhaya (1993) to find the response of railway tracks on elastic subgrade. Vehicle models with seven and twelve degrees of freedom were developed by Wang *et al.* (1993) according to H20-44 and HS20-44 which are major design vehicles in the American Association of State Highway and Transportation Officials (AASHTO). However, analysis of vehicle motions was confined to rigid modes only. Other notable works in bridge vehicle interaction dynamics that include various dynamic properties of rigid vehicle have been reported by Chen and Cai (2004), Law and Zhu (2005) and Zhang *et al.* (2006), Green and Cebon (1997).Various works on bridge vehicle interaction on multi-span bridges have been reported by Huang and Wang (1992), Huang *et al.* (1992), Wang (1992) and Ichikawa *et al.* (2000). Numerical techniques for solving the finite element model with rigid vehicle have been adopted.

Interests in research on bridge-vehicle interaction dynamics are still growing because of several complexities in modeling and uncertainties in excitation. In the last decade, researchers have undertaken more and more complex problems and attempted to solve by newer methodology taking into consideration of support flexibility and non uniform cross section. A vehicle-track-bridge interaction element considering vehicle's pitching effect has been developed by Lou (2005). Experimental results and its comparison with Finite Element model analysis of vehicle-bridge interaction problem has been presented by Brady *et al.* (2006). Rigid model of vehicle has been considered in the study to determine set of critical velocity associated with peaks of dynamic amplification factor. Multiple reasonance response of railway bridge has been investigated by Yau and Yang (2004). A vehicle bridge interaction process has been simulated with MATLAB Simulink by Harris *et al.* (2007) to find out bridge-friendly damping control strategy with a tractor semi-trailer vehicle model. Very recently, some interesting studies of bridge-vehicle or road-vehicle coupled dynamics includes stochastic numerics and discrete integration schemes for digital simulation of road-vehicle system by Wedig (2012), application of spectral stochastic finite element by Wu and Law (2012) and use of spectral matrix operator for direct solution of stochastic coupled differential equations by Kozar and Malic (2013). Concrete bridge degeneration and development of fatigue cracks over long period of service life affects the dynamic characteristics of bridge. Wang *et al.* (2012) studied time frequency characteristics of a concrete bridge with breathing cracks using Hilbert-Huang and wavelet transform techniques. Yang et.al (2012) has investigated the effect of road unevenness on the response of a moving vehicle with an aim to identify the bridge frequencies using both numerical and analytical methods. The analytical theory has been extended for two vehicles from which it was concluded that the vehicle spacing is not a key parameter to identify bridge frequencies, rather smooth movement of vehicle is necessary for clearly identifying first few bridge frequencies. The studies reported by past researchers have significantly improved the understanding of complex problem in vehicle-bridge interactions. However, in most of the studies, vehicle model has been assumed as lumped masses with rigid link connected by suspension elements exhibiting various discrete degrees of freedom. In the modern days, characteristics of vehicles have greatly changed due to incorporation of larger pay load and for increasing demand of traffic. In the past, vehicles have been modeled by a rigid 2D or 3D system having degrees of freedom in bounce, pitch and roll. However, due to long and slender vehicle plying frequently over the bridges, there is a need to consider flexibility in the vehicle model and to examine the effect of flexible modes of vehicle on the dynamics of bridge.

With this in mind, present study has been conducted to find out the response statistics of single span bridge due to movement of flexible vehicle. By the term 'flexible vehicle', it is understood here that flexural modes have been included in addition to rigid body modes. The bridge has been considered to be under independent transverse bending as well as under torsional excitation arising out of the eccentric path of the vehicle. Non homogeneous profile of deck surface has been incorporated in the study by considering a deterministic mean surface super imposed by zero mean random process. Such formulation can take care of defects in surface finishing, construction joints, potholes, bump, approach slab settlement etc. In the present study, approach slab settlement and pre cambered deck surface has been considered. The deck surface roughness height variation has been transformed to time domain input using a general vehicle forward motion pattern. Newmark-β method has been used for the numerical integration of bridge-vehicle system equation. The different parameters of the bridge and vehicle influence the dynamic behavior. Among theses, speed of the vehicle, vehicle configuration, weight and deck unevenness are the most contributing ones. Most of the design codes of bridge recommend the use of dynamic amplification factor to take dynamic effect into consideration. Simplified formulae involving bridge span only exists in majority of the bridge codes (Coussey *et al*. 1989), which does not reflect the effect of true vehicle pattern, bridge pavement unevenness and vehicle speed. It may be mentioned that dynamic loads do not lead to major bridge damage, except in resonance but they contribute to continuous degradation of bridge, thereby increasing necessity of bridge maintenance. Examining the effects of these factors on the bridge response is practically significant for life safety of the bridge, periodic maintenance as well as for vehicle maintenance and operational cost. The observations from different parametric studies have been presented to give insight to the structural behavior.

2. Mathematical model

The bridge-vehicle model has been shown in Fig. 1. The bridge has been modeled as a uniform beam with simply supported end conditions. The mass, stiffness and damping are assumed to be uniform along the span of bridge. Due to eccentricity of the vehicle path, the bridge is subjected to flexure as well as torsion. The bridge deck is uneven which has been realized as non homogeneous process in spatial domain. This is represented by a function $h(x)$.
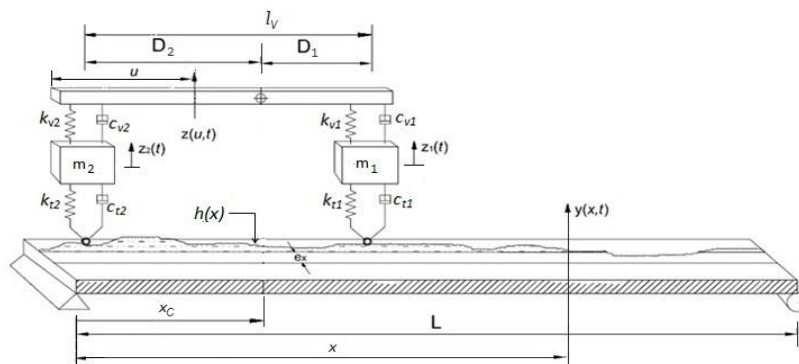

Fig. 1 Bridge-vehicle system model

2.1 Equation of motion of Vehicle

Vehicle body has been idealized as Euler-Bernoulli beam of length l_v. The behavior of suspension systems consisting of spring and dashpot are assumed as linear. The governing differential equation of motion of the vehicle deflection can be expressed as

$$E_v I_v \frac{\partial^4 z(u,t)}{\partial u^4} + C_v \frac{\partial z(u,t)}{\partial t} + m_v \frac{\partial^2 z(u,t)}{\partial t^2} = f_v(u,t) \tag{1}$$

in which m_v, $E_v I_v$ and C_v denote the mass per unit length, flexural rigidity and viscous damping per unit length of the vehicle body, $z(u,t)$ represents vertical deflection of the vehicle body measured at location u from the reference point (taken at the left end of the vehicle) at time instant t. The impressed vertical force on the vehicle body is given by

$$f_v(u,t) = \left[k_{v1} \{ z(u,t) - z_1(t) \} + c_{v1} \{ \dot{z}(u,t) - \dot{z}_1(t) \} \right] \delta(u - u_1)$$
$$+ \left[k_{v2} \{ z(u,t) - z_2(t) \} + c_{v2} \{ \dot{z}(u,t) - \dot{z}_2(t) \} \right] \delta(u - u_2) \tag{2}$$

where u_1 and u_2 represent the location of the attachment point of vehicle suspension from the reference point; z_1 and z_2 denote the vertical displacement of front and rear wheel masses respectively. k_{v1} and k_{v2} are the front and rear vehicle suspension stiffness respectively; c_{v1} and c_{v2} represent damping for vehicle front and rear suspension respectively.

The equation of motion for the front un-sprung mass is given by

$$m_1 \ddot{z}(t)_1 + k_{t1} \{ z_1(t) - y(x_1,t) - h(x_1) \} + k_{v1} \{ z_1(t) - z(u_1,t) \} + c_{v1} \{ \dot{z}_1(t) - \dot{z}(u_1,t) \}$$
$$+ c_{t1} [\dot{z}_1(t) - \frac{D}{Dt} \{ y(x_1,t) + h(x_1) \}] = 0 \tag{3}$$

The equation of motion for the rear un-sprung mass is given by

$$m_2 \ddot{z}_2(t) + k_{t2} \{ z_2(t) - y(x_2,t) - h(x_2) \} + k_{v2} \{ z_2(t) - z(u_2,t) \} + c_{v2} \{ \dot{z}_2(t) - \dot{z}(u_2,t) \}$$
$$+ c_{t2} [\dot{z}_2(t) - \frac{D}{Dt} \{ y(x_2,t) + h(x_2) \}] = 0 \tag{4}$$

where, m_1 and m_2 are front and rear wheel mass respectively, k_{t1}, k_{t2} are front and rear suspension stiffness respectively; c_{t1}, c_{t2} are front and rear suspension damping respectively. $h(x_1)$ and $h(x_2)$ represents the non homogeneous deck profile under the front and rear wheels respectively. $y(x_1,t)$ and $y(x_2,t)$ are bridge displacements under front and rear wheels respectively at any instant of time t. $z(u_1,t)$ and $z(u_2,t)$ represents vehicle body deflection at the front and rear wheels position at any instant of time t. u_1 and u_2 is the location of wheel from the end of the vehicle body. The single over dot (.) denotes first time derivative. Coriolis forces that arise due to rolling of wheel on the deflected profile of the bridge has been considered in the equation of motion using total derivative operator D/Dt (with $Dy/Dt=(\partial y/\partial x)(\partial x/\partial t) + \partial y/\partial t$). (Fryba 1996, Nasrellah and Monahar 2010)

2.2 Equation of motion of bridge

It is assumed that for symmetrical cross section (symmetrical about vertical axis), bending and torsion of the bridge would be independent under vertically applied live load. Thus governing

differential equation of motion of the bridge in flexure can be expressed as

$$E_b I_b \frac{\partial^4 y(x,t)}{\partial x^4} + C_b \frac{\partial y(x,t)}{\partial t} + m_b \frac{\partial^2 y(x,t)}{\partial t^2} = f_b(x,t)$$ (5)

in which m_b, $E_b I_b$ and C_b represents the mass per unit length, flexural rigidity and viscous damping per unit length of bridge. The impressed vertical force $f_b(x,t)$ on the bridge due to vehicle interaction is given by

$$f_b(x,t) = -\left[k_{t1}\{z_1(t) - y(x,t) - h(x)\} + c_{t1}\left\{ \dot{z}_1(t) - \frac{D}{Dt}[y(x,t) + h(x)] \right\} \right] \delta(x - x_1)$$

$$- \left[k_{t2}\{z_2(t) - y(x,t) - h(x)\} + c_{t2}\left\{ \dot{z}_2(t) - \frac{D}{Dt}[y(x,t) + h(x)] \right\} \right] \delta(x - x_2)$$

$$- \{m_1 + \frac{1}{2}m_v l_v\}g\delta(x - x_1) - \{m_2 + \frac{1}{2}m_v l_v\}g\delta(x - x_2)$$ (6)

$$+ m_1 \frac{D^2}{Dt^2}[y(x,t) + h(x)]\delta(x - x_1) + m_2 \frac{D^2}{Dt^2}[y(x,t) + h(x)]\delta(x - x_2)$$

where g is the acceleration due to gravity. The governing differential equation of the bridge in torsion can be written as

$$G_b J_b \frac{\partial^2 \gamma(x,t)}{\partial x^2} - C_{bT} \frac{\partial \gamma(x,t)}{\partial t} - I_b \frac{\partial^2 \gamma(x,t)}{\partial t^2} = f_T(x,t)$$ (7)

in which I_b, $G_b J_b$, C_{bT} and $\gamma(x,t)$ represents the mass moment of inertia per unit length, torsional rigidity, distributed viscous damping to rotational motion and torsional function of bridge. J_b is torsional constant, G_b is the shear modulus of beam material. $f_T(x,t)$ is the torque produced in the bridge cross section due to eccentric loading which is given by

$$f_T(x,t) = -\left[k_{t1}\{z_1(t) - y(x,t) - h(x)\} + c_{t1}\left\{ \dot{z}_1(t) - \frac{D}{Dt}[y(x,t) + h(x)] \right\} \right] e_x \delta(x - x_1)$$

$$- \left[k_{t2}\{z_2(t) - y(x,t) - h(x)\} + c_{t2}\left\{ \dot{z}_2(t) - \frac{D}{Dt}[y(x,t) + h(x)] \right\} \right] e_x \delta(x - x_2)$$ (8)

$$- \{m_1 + \frac{1}{2}m_v l_v\}g\, e_x \delta(x - x_1) - \{m_2 + \frac{1}{2}m_v l_v\}g\, e_x \delta(x - x_2)$$

$$+ m_1 \frac{D^2}{Dt^2}[y(x,t) + h(x)]e_x \delta(x - x_1) + m_2 \frac{D^2}{Dt^2}[y(x,t) + h(x)]e_x \delta(x - x_2)$$

The parameter e_x in Eq. (8) denotes the eccentricity of vehicle wheels from the centre line of bridge deck.

2.3 Bridge deck roughness

In the present study we introduce a form of road roughness, which is non homogeneous in space even though vehicle velocity is constant, by adopting following relation

$$h(x) = h_m(x) + \sum_{s=1}^{N} \varsigma_s \cos(2\pi \Omega_s x + \theta_s)$$ (9)

where $h_m(x)$ is a deterministic mean which represents construction defects, expansion joints, created pot holes, approach slab settlement, development of corrugation etc., ς_s is the amplitude of cosine wave, Ω_s is the spatial frequency (rad/m) within the interval [Ω_L Ω_U] in which power spectral density is defined. Ω_L and Ω_U are lower and upper cut off frequencies. The deck roughness is a Gaussian process (Shinozuka 1971) with a random phase angle θ_s uniformly distributed from 0 to 2π. N is the number of terms used to build up the road surface roughness. The parameters ς_s and Ω_s are computed as

$$\varsigma_s = \sqrt{2S(\Omega_s)\Delta\Omega}$$
$$\Omega_s = \Omega_L + (s - 1/2)\Delta\Omega$$
$$\Delta\Omega = (\Omega_U - \Omega_L)/N$$
(10)

in which $S(\Omega_s)$ is the power spectral density function (m³/rad) taken from the reference (Huang and Wang 1992) modifying the same with addition of one term in denominator so that the function exists when $\Omega \rightarrow 0$.

$$S(\Omega) = S(\Omega_0) \times \frac{\Omega^2_0}{\Omega_s^2 + \Omega^2_L}$$
(11)

In the above equation, $\Omega_0 = 1/2\pi$ rad/m has been taken. The spatial frequency Ω (rad/m) and temporal frequency ω (rad/s) for the surface profile is related with the vehicle speed V (m/s) as $\omega = \Omega V$. In the present study, vehicle forward velocity has been assumed as constant.

In the present study two types of deterministic mean profile - (i) pre cambering of bridge in the form of shallow parabolic, (ii) approach slab settlement as ramp function have been considered. The analytical form representing deterministic mean profile are given below

For case (i), $$h_m(x) = \frac{4h_0}{L^2} x(L - x) , \ 0 \leq x \leq L$$
(12)

For case (ii), $$h_m(x) = \frac{h_1}{L_r} x , 0 \leq x \leq L_r$$
$$= h_1 , x \geq L_r$$
(13)

where h_0 is the central rise of mean parabolic surface, h_1 represents approach slab settlement , L_r is the ramp length and L is the bridge span.

2.4 Discretization of flexible vehicle equation of motion

As mentioned earlier vehicle body has been modeled as free-free beam which has two rigid modes and n_v number of elastic bending modes. It can be shown that when the translation of the mass centroid and the rotational motion about the mass centroid are considered, the two motions are orthogonal with respect to each other and with respect to the elastic modes (Hodges and Pierce, 2002). Thus total displacement of these rigid body degrees of freedom and elastic modes can be described by

$$z(u,t) = \sum_{j=-1}^{\infty} \phi_{vj}(u)\eta_j(t) \tag{14}$$

where $\phi_{vj}(u)$ is the vehicle mode shapes, the subscript v denotes vehicle, $\eta_j(t)$ is the time dependent generalized coordinate, j is the mode number; $j=-1, 0$ are taken to denote rigid body translatory and pitching mode, $j=1,2,3\ldots n_v$ represent elastic mode sequence of free-free beam; n_v is the number of significant flexible vehicle body modes. Thus two rigid body modes can be written as

$$\phi_{-1} = 1; \quad \phi_0 = u - D_2 \tag{15}$$

D_2 is a distance of vehicle centre of gravity from the trailing edge as given Fig. 1.
The elastic bending modes of free-free beam for $j=1,2,3\ldots$ are given by (Inman 2001)

$$\phi_{vj} = \sin(\alpha_j u) + \sinh(\alpha_j u) + \beta_j[\cos(\alpha_j u) + \cosh(\alpha_j u)]; \quad \beta_j = \frac{\cos(\alpha_j l_v) + \cosh(\alpha_j l_v)}{\sin(\alpha_j l_v) + \sinh(\alpha_j l_v)} \tag{16}$$

where corresponding non dimensional frequency parameters $\alpha_j l_v$ can be related to circular natural frequency as

$$\omega_{vj} = \alpha_j^2 \sqrt{\frac{E_v I_v}{m_v l_v^4}} \tag{17}$$

Substituting Eq. (14) in Eq. (1) and multiplying both sides of the equation by $\phi_{vk}(u)$ and then integrating with respect to u from 0 to l_v along with orthogonality conditions, the equation of motion can be discretized as

$$\ddot{\eta}_j(t) + 2\xi_{vj}\omega_{vj}\dot{\eta}_j(t) + \omega_{vj}^2\eta_j(t) = Q_{vj}(t) \quad ; \quad j = -1,0,1,2\ldots \tag{18}$$

Generalized force $Q_{vj}(t)$ in the jth mode acting on the vehicle is given as,

$$Q_{vj}(t) = \frac{1}{M_{vj}} \int_0^{l_v} f_v(u,t)\phi_j(u)du \tag{19}$$

in which generalized mass M_{vj} in the jth mode is given by

$$M_{vj} = \int_0^{l_v} m_v \phi_{vj}^2(u)du \tag{20}$$

Making use of Eqs. (2) and (14) in Eq. (19) and integrating the expression using the property of Dirac delta function, one has the following expression for generalized force.

$$Q_{vj}(t) = \frac{1}{M_{vj}}[k_{v1}\{z_1(t) - \sum_{j=-1}^{n_v}\phi_j(u_1)\eta(t)\}\phi_j(u_1) + c_{v1}\{\dot{z}_1(t) - \sum_{j=-1}^{n_v}\phi_j(u_1)\dot{\eta}(t)\}\phi_j(u_1)$$

$$k_{v2}\{z_2(t) - \sum_{j=-1}^{n_v}\phi_j(u_2)\eta(t)\}\phi_j(u_2) + c_{v2}\{\dot{z}_2(t) - \sum_{j=-1}^{n_v}\phi_j(u_2)\dot{\eta}(t)\}\phi_j(u_2)] \tag{21}$$

It may be mentioned that infinite number of modes are possible in continuous system considered in the present study. However, for practical implementation only first n_v modes of

vehicle body has been included.

2.5 Discretization of Bridge equation of motion

Using mode superimposition principle, the bridge deflection in flexure can be written as

$$y(x,t) = \sum_{k=1}^{\infty} \phi_{bk}(x)q_k(t) \tag{22}$$

where $k=1,2,3\ldots\ldots n_b$; n_b represents number of significant bridge flexural mode. Subscript b represents bridge, $\phi_{bk}(x)$ is the flexural mode of the beam for simply supported boundary condition corresponding to natural frequency ω_{bk} and $q_k(t)$ are generalized co-ordinates in k^{th} mode (Inman 2001)

Now, substituting Eq. (22) in Eq. (5) and multiplying both sides of the equation by $\phi_{bj}(x)$ and then integrate with respect to x from 0 to L with the use of orthogonality conditions, the equation of motion can be discretized in normal co-ordinates as

$$\ddot{q}_k(t) + 2\xi_{bk}\omega_{bk}\dot{q}_k(t) + \omega_{bk}^2 q_k(t) = Q_{bk}(t) \quad ; k = 1,2,3\ldots n_b \tag{23}$$

The generalized force $Q_{bk}(t)$ in the kth mode of bridge in flexure is given as,

$$Q_{bk}(t) = \frac{1}{M_{bk}} \int_0^L f_b(x,t)\phi_{bk}(x)dx \tag{24}$$

in which generalized mass M_{bk} in the kth mode is given by

$$M_{bk} = \int_0^L m_b \phi_{bk}^2(x)dx \tag{25}$$

The generalized force in the kth of mode of bridge transverse vibration has been worked out as

$$Q_{bk}(t) = -\frac{1}{M_{bk}}\Bigg[k_{t1}\bigg\{ z_1(t) - \sum_{k=1}^{n_b}\phi_{bk}(x_1)q_k(t) - h(x_1)\bigg\}\phi_{bk}(x_1) + k_{t2}\bigg\{ z_2(t) - \sum_{k=1}^{n_b}\phi_{bk}(x_2)q_k(t) - h(x_2)\bigg\}\phi_{bk}(x_2)$$

$$+ c_{t1}\bigg\{ \dot{z}_1(t) - V\sum_{k=1}^{n_b}\phi_{bk}'(x_1)q_k(t) - V\sum_{k=1}^{n_b}\phi_{bk}(x_1)\dot{q}_k(t) - Vh'(x_1)\bigg\}\phi_{bk}(x_1) - \{m_1 + \frac{1}{2}m_v l_v\}g\phi_{bk}(x_1)$$

$$+ c_{t2}\bigg\{ \dot{z}_2(t) - V\sum_{k=1}^{n_b}\phi_{bk}'(x_2)q_k(t) - V\sum_{k=1}^{n_b}\phi_{bk}(x_2)\dot{q}_k(t) - Vh'(x_2)\bigg\}\phi_{bk}(x_2) - \{m_2 + \frac{1}{2}m_v l_v\}g\phi_{bk}(x_2)$$

$$+ m_1\bigg\{ \sum_{k=1}^{n_b}\phi_{bk}(x_1)\ddot{q}_k(t) + 2V\sum_{k=1}^{n_b}\phi_{bk}'(x_1)\dot{q}_k(t) + V^2\sum_{k=1}^{n_b}\phi_{bk}''(x_1)q_k(t) + 4Vh''(x_1)\bigg\}\phi_{bk}(x_1)$$

$$+ m_2\bigg\{ \sum_{k=1}^{n_b}\phi_{bk}(x_2)\ddot{q}_k(t) + 2V\sum_{k=1}^{n_b}\phi_{bk}'(x_2)\dot{q}_k(t) + V^2\sum_{k=1}^{n_b}\phi_{bk}''(x_2)q_k(t) + 4Vh''(x_2)\bigg\}\phi_{bk}(x_2)\Bigg] \tag{26}$$

Repeating the similar steps, the discredited bridge equation for torsion in normal co-ordinate can be expressed as

$$\ddot{\gamma}_l(t) + 2\xi_{Tl}\omega_{Tl}\dot{\gamma}_l(t) + \omega_{Tl}^2\gamma_l(t) = Q_{Tl}(t); \quad (l = 1,2,3\ldots n_T) \tag{27}$$

where n_T represents number of bridge torsional modes considered, ω_{Tl} and ξ_{Tl} are the natural

frequency and modal damping coefficient of lth mode in torsion respectively. The generalized torque in the lth mode is given by

$$Q_{Tl}(t) = \frac{1}{M_{Tl}} \int_0^L f_T(x,t)\phi_{Tl}(x)dx \tag{28}$$

The torsional natural frequency ω_{Tl} and the corresponding mode Φ_{Tl} for the given simply supported boundary conditions for no warping restrains have been taken from reference (Inman 2001). The generalized mass moment of inertia M_{Tl} in the lth mode is given by

$$M_{Tl} = \int_0^L I_b\phi_{Tl}^2(x)dx \tag{29}$$

The generalized torque in the lth mode can be expressed as

$$
\begin{aligned}
Q_{Tl}(t) = -\frac{e_x}{M_{Tl}} \Bigg[&k_{t1}\left\{z_1(t) - \sum_{l=1}^{n_T}\phi_{Tl}(x_1)\gamma_l(t) - h(x_1)\right\}\phi_{Tl}(x_1) + k_{t2}\left\{z_2(t) - \sum_{l=1}^{n_T}\phi_{Tl}(x_2)\gamma_l(t) - h(x_2)\right\}\phi_{Tl}(x_2) \\
&+ c_{t1}\left\{\dot{z}_1(t) - V\sum_{l=1}^{n_T}\phi_{Tl}'(x_1)\gamma_l(t) - V\sum_{l=1}^{n_T}\phi_{Tl}(x_1)\dot{\gamma}_l(t) - Vh'(x_1)\right\}\phi_{Tl}(x_1) - \{m_1 + \tfrac{1}{2}m_v l_v\}g\phi_{Tl}(x_1) \\
&+ c_{t2}\left\{\dot{z}_2(t) - V\sum_{l=1}^{n_T}\phi_{Tl}'(x_2)\gamma_l(t) - V\sum_{l=1}^{n_T}\phi_{Tl}(x_2)\dot{\gamma}_l(t) - Vh'(x_2)\right\}\phi_{Tl}(x_2) - \{m_2 + \tfrac{1}{2}m_v l_v\}g\phi_{Tl}(x_2) \\
&+ m_1\left\{\sum_{l=1}^{n_T}\phi_{Tl}(x_1)\ddot{\gamma}_l(t) + 2V\sum_{l=1}^{n_T}\phi_{Tl}'(x_1)\dot{\gamma}_l(t) + V^2\sum_{l=1}^{n_T}\phi_{Tl}''(x_1)\gamma_l(t) + 4Vh''(x_1)\right\}\phi_{Tl}(x_1) \\
&+ m_2\left\{\sum_{l=1}^{n_T}\phi_{Tl}(x_2)\ddot{\gamma}_l(t) + 2V\sum_{l=1}^{n_T}\phi_{Tk}'(x_2)\dot{\gamma}_l(t) + V^2\sum_{k=1}^{n_T}\phi_{Tk}''(x_2)\gamma_l(t) + 4Vh''(x_2)\right\}\phi_{Tl}(x_2) \Bigg]
\end{aligned}
\tag{30}
$$

2.6 Method of solution

The system of Eqs. (3), (4), (18), (23) and (27) are coupled second order ordinary differential equations. In general for continuous system like the ones (vehicle and bridge), presented in the paper infinite number of modes exists. However, for practical applications, modes have to be truncated to a finite size. Let n_v, n_b and n_T be number of significant modes of vehicle motion, bridge flexural and torsional vibration respectively. The number of coupled equations becomes $n=2+n_v+n_b+n_T$. The system equations can be expressed in matrix notation as

$$[M]\{\ddot{r}(t)\} + [C]\{\dot{r}(t)\} + [K]\{r(t)\} = \{F(t)\} \tag{31}$$

where $\{r(t)\}=\{\eta_1(t),\ \eta_1(t),\ldots,\eta_{nv}(t),\ z_1(t), z_2(t),\ q_1(t), q_2(t)\ldots, q_{nb}(t), \gamma_1(t),\ \gamma_2(t)\ldots,\ \gamma_{nT}(t)\}^{\text{T}}$ is the response vector, $\{F(t)\}$ is the generalized force vector and, $[M]$, $[C]$ and $[K]$ are system mass, damping and stiffness matrix respectively. Any direct integration method can be used to solve Eq. (31). In the present study, the Newmark-β method has been adopted (Bathe and Wilson 1987). The force vector $\{F(t)\}$ is a function of deck roughness and its derivative which are considered as a random process in the study. In the present paper, response time histories (sample output) have been generated corresponding to each simulated sample of surface roughness (sample input) which

is the main source of excitation. Collecting all such output samples, the ensemble of random process can be written as

$$\{Y(t)\} = \{y_1(t), y_2(t),..., y_n(t)\} \tag{32}$$

where $y_j(t)$ is the jth sample time history in the ensemble set. At each time step t_k, $y_j(t_k)$ is the jth realization of random process $Y(t_k)$. Thus one can find the mean $\mu_Y(t_k)$ and standard deviation $\sigma_Y(t_k)$ of the random process $Y(t)$ at any time step t_k, using the theory of statistics (Nigam 1983) as

$$\mu_Y(t_k) = \frac{1}{N_s} \sum_{j}^{Ns} y_j(t_k) \tag{33}$$

$$\sigma_Y(t_k) = \sqrt{\frac{1}{N_s - 1} \sum_{j=1}^{Ns} \{y_j(t_k) - \mu_Y(t_k)\}^2} \tag{34}$$

in which N_s represents number of time history samples inside the ensemble set $\{Y(t)\}$.

3. Result and discussion

The following system data have been adopted to generate numerical results and to conduct parametric study. A RC slab –Girder Bridge of span (L): 20 m; Three Longitudinal girders along the span and three cross girders at mid span and at supports are provided in bridge. The lane width: 8.6 m, Deck Thickness: 200 mm, concrete characteristic strength 25 N/mm^2. The cross section of the bridge is shown in Fig. 2. A Finite Element (FE) model of bridge in SAP2000 commericial software is first developed using above details of the bridge so as to match the fundamental natural frequency and first modal damping ratio of the simply supported beam model of T-beam bridge. The sectional properties of FE model is then used in the present analytical program of the bridge. The following physical parameters are finally selected for the beam model to represent a T-beam RC concrete bridge:

Mass (m_b): 11.15x10^3 kg/m, flexural rigidity (E_bI_b):3.7x10^{10} N-m^2, torsional rigidity (G_bJ_b): 1.695x10^{10} N-m^2. It may be noted that above sectional parameters in the beam model of bridge has been found from the FE model of bridge in SAP 2000 software after tuning the fundamental natural frequency and first modal damping of the both the analytical and FE model of bridge.

Vehicle parameters: A long vehicle carrying heavy load often crossing the bridge has been chosen to illustrate the present approach. The standards of vehicle are different from the live load prescribed by bridge code. In the present study, we use a Vehicle type: TATA 3516C-EX as shown in Figs. 3 and 4. This has been idealized as Euler Bernoulli beam in present formulation. Following are the important physical parameters pertaining to vehicle: length (l_v): 12 m, flexural rigidity (E_vI_v): 5.3x10^6 N-m^2, mass per unit length (m_v): 1500 kg/m, front and rear wheel masses (m_{w1},m_{w2}): 800 kg each, Suspension stiffness front and rear (k_{v1}, k_{v2}): 3.6x10^7 N/m, Suspension damping front and rear (c_{v1}, c_{v2}): 7.2x10^4 N-sec/m, front and rear tyre stiffness (k_{t1}, k_{t2}): 0.9x10^7 N/m, front and rear tyre damping (k_{t1}, k_{t2}): 0.7x10^4 N-sec/m.
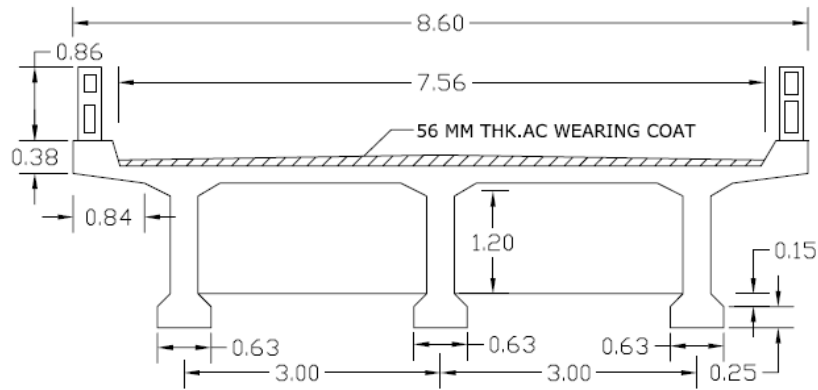
Fig. 2 Cross section of T-beam bridge (All dimensions are in meter)
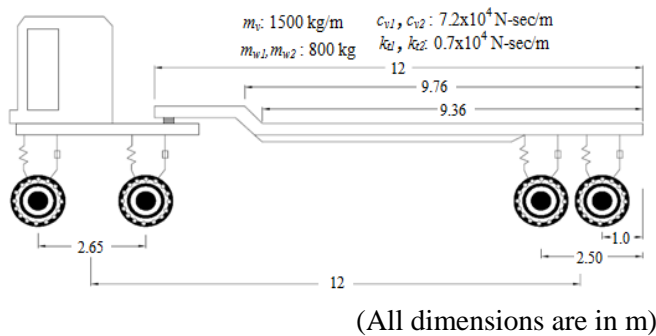
(All dimensions are in m)
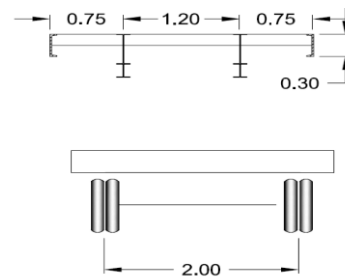
Fig. 3 Longitudinal section of vehicle   Fig. 4 Vehicle cross section

3.1 Effect of vehicle speed on response statistics

Effect of vehicle speed on the mean response of bridge has been studied by varying vehicle speed from 50 km/h to 80 km/h. Fig. 5 shows mean displacement and Fig. 6 shows standard deviation of the displacement for surface roughness of category-poor as per ISO standard (ISO 8606, 1995) along with mean surface profile in the form of shallow parabola of central rise 5 mm from datum. Figs. 7 and 8 show the mean and standard deviation of mid span displacement when settlement of 5 mm exists at bridge approach slab.

Result shows that frequency of the bridge mid span displacement time history has been fashioned due to change of vehicle velocity. This is expected for a linear time variant system since as the velocity increases, temporal frequency of excitation, also increases. This produces left shift of the displacement peak as observed in the Fig. 5. The increase of peak magnitudes with increase of velocity has also been noticed in the present case for a range of velocity considered in the study. Earlier researchers have also noted similar trend on the peak response due to the effect of increased velocity on the bridge maximum displacement (Chang and Lee 1994, Esmailzadeh and

Jalii 2003). In some cases (Mallic and Kozar 2012), high speed movement of vehicle seems to produce reverse trend in stiffened plate, which might be due to the fact that the stiffened plate has very less time to react to the excitation, as the load passes very rapidly. No definite pattern is discernible in the standard deviation plot in Fig.6. Although, the magnitudes of standard deviation are insignificant for practical purpose, magnitude of the coefficient of variation of peak displacement, velocity and accelerations are found to be 0.11, 0.183 and 0.105 respectively. It may be mentioned that dynamic loads do not lead to major bridge damage, except in resonance but they contribute to continuous degradation of bridge increasing necessity of bridge maintenance.
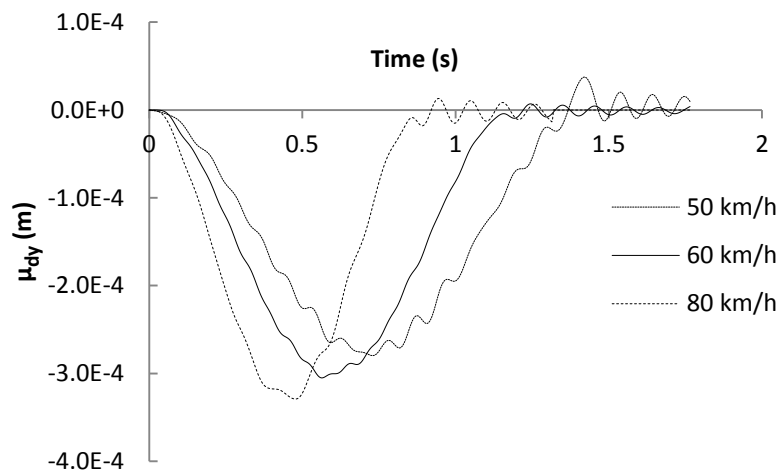
Fig. 5 Mean of bridge mid span displacement for different vehicle speed with mean surface as shallow parabola of central rise 5 mm
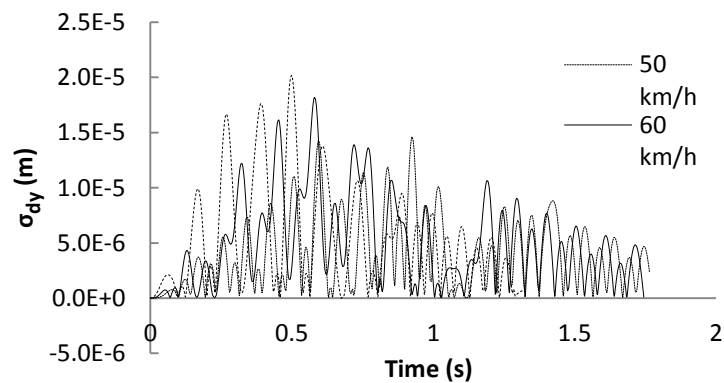
Fig. 6 Standard deviation of bridge mid span displacement for different vehicle speed with mean surface as shallow parabola of central rise 5 mm
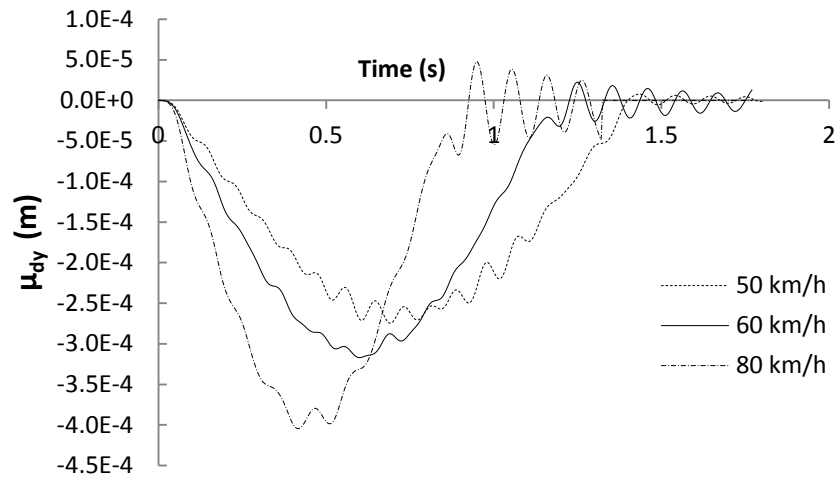
Fig. 7 Mean of bridge mid span displacement for different vehicle speed with 5mm approach slab settlement
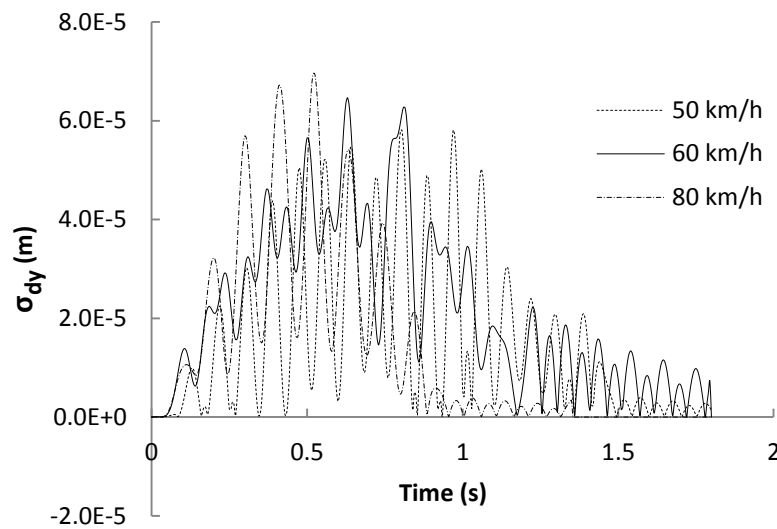
Fig. 8 Standard deviation of bridge mid span displacement for different vehicle speed with 5 mm approach slab settlement

3.2 Effect of approach slab settlement

Effect of support slab settlement on the bridge response has been studied for different settlement magnitudes. Bridge mid span response subjected to 12 m vehicle axle spacing with 60 km/h speed are shown in Fig. 9 and the corresponding standard deviations are given in Fig. 10.

Only 1.2% to 3.5% increment in the bridge response has been found for approach settlement up to 2 mm. However, considerable increment in the response ranging from 14% to 34.3% has been observed when settlement increases from 5 mm to 9 mm.
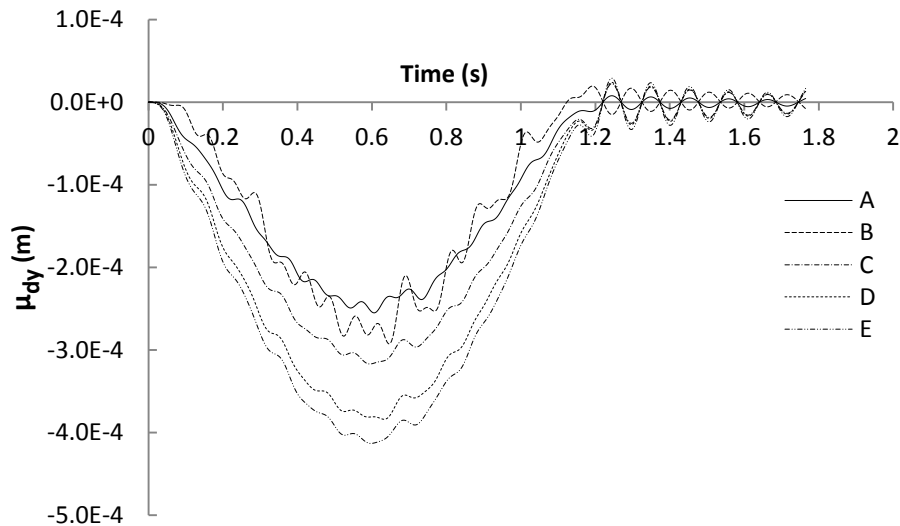
Fig. 9 Mean displacement of bridge at mid span for different settlement (A) without approach slab settlement, (B) 2 mm settlement, (C) 5 mm settlement, (D) 7 mm settlement, (E) 9 mm settlement
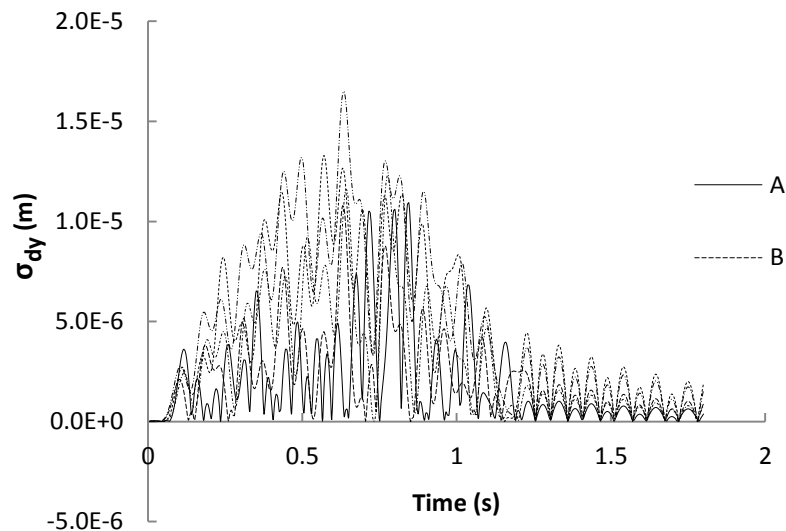
Fig. 10 Standard deviation of bridge mid span deflection for different settlement (A) zero settlement, (B) 2 mm settlement, (C) 5 mm settlement, (D) 7 mm settlement, (E) 9 mm settlement

3.3 Effect of Vehicle flexibility on mean and standard deviation

The contribution of significant number of structural mode of vehicle on bridge response has been examined in a time history plot of mean and standard deviation (Figs. 11 and 12) of the bridge mid span deflection due to moving vehicle. The comparison of peak responses have been shown in the bar diagrams in Figs. 13 and 14. It may be seen that inclusion of bending modes of the vehicle reduces the response magnitude of the bridge as compared to that caused by only rigid body motion of the vehicle to the extent of 30-37% in the present examples. The contribution of first five structural bending modes of the vehicle has been found adequate in response calculation approach outlined in the present study. Figs. 15 and 16 show the comparison of mean and standard deviation of imposed force on the bridge due to passage of a rigid vehicle with those of flexible vehicle. It reveals that when structural bending modes are considered, the imposed force on the bridge is less. This may be attributed to the fact that a part of total strain energy has been utilized in bending of elastic vehicle body as compared to rigid beam, which reduces imposed force on the bridge and hence magnitude of the displacement.
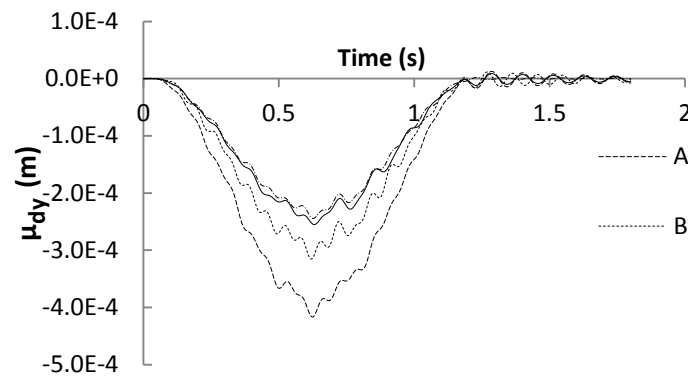

Fig. 11 Mean displacement of bridge at mid span, (A) Rigid vehicle, (B) flexible vehicle only with first structural mode, (C) flexible vehicle with first three structural modes, (D) flexible vehicle with first five structural modes
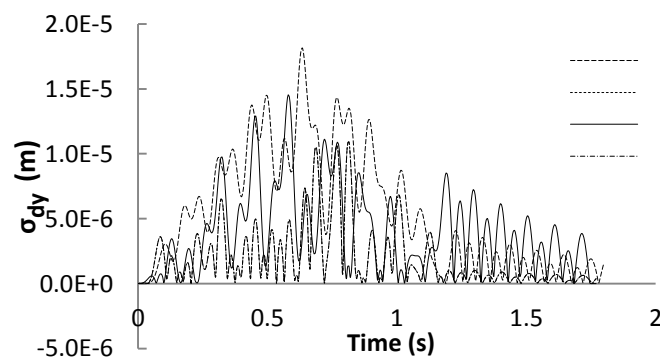

Fig. 12 Standard deviation of displacement at mid span   (A) Rigid vehicle, (B) flexible vehicle only with first structural mode (C) flexible vehicle with first three structural modes, (D) flexible vehicle with first five structural modes

3.4 Effect of eccentricity of vehicle path on mean and standard deviation

The effect of eccentricity on the bridge loading has been studied by varying the loading position from the centre of the bridge width. In the result shown in Figs. 17 and 18, 6% to 8% increment in the bridge dynamic responses has been observed as the eccentricity varies from 0.5 m to 1.5 m. The results under this section are obtained taking vehicle forward velocity as 60 km/h.
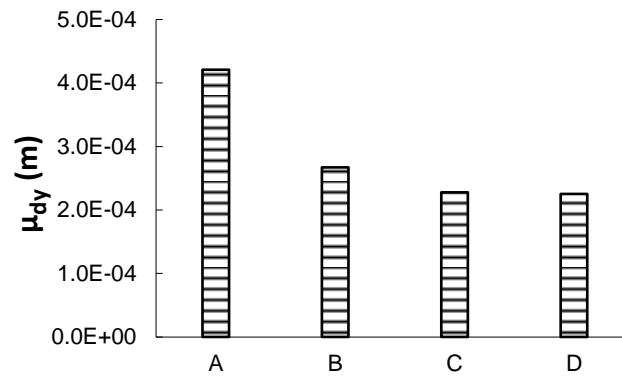

Fig. 13 Maximum mean displacement of bridge at mid span, (A) Rigid vehicle, (B) flexible vehicle only with first structural mode, (C) flexible vehicle with first three structural modes, (D) flexible vehicle with first five structural modes
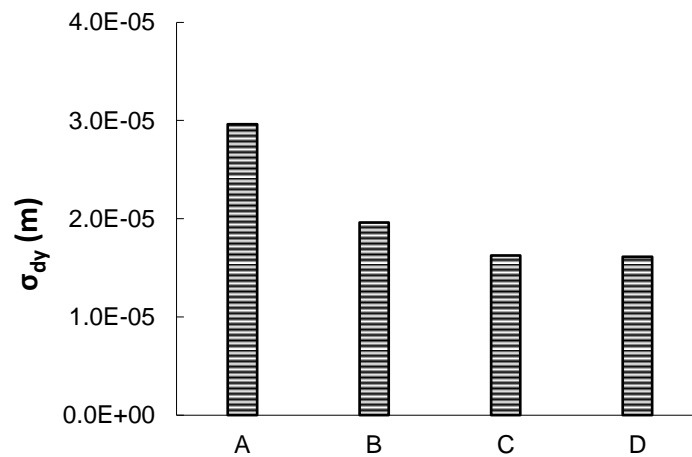

Fig. 14 Maximum standard deviation of displacement at mid span   (A) Rigid vehicle, (B) flexible vehicle only with first structural mode (C) flexible vehicle with first three structural modes, (D) flexible vehicle with first five structural modes
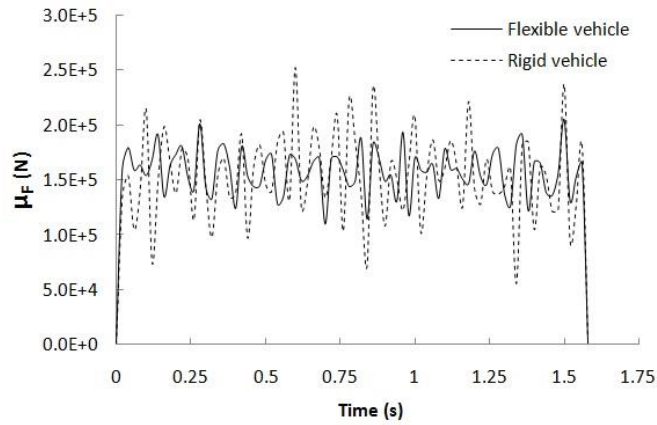
Fig. 15 Mean of imposed force time history of the bridge due to passage of rigid and flexible vehicle
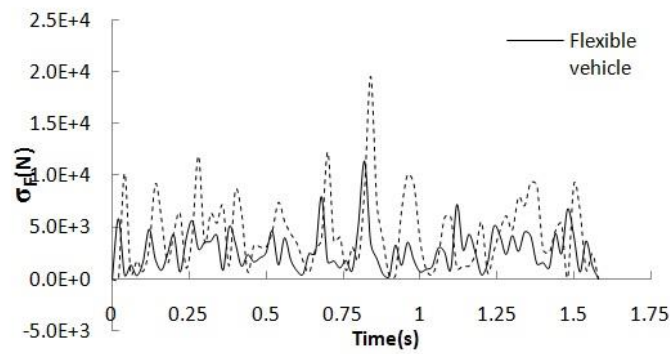

Fig. 16 Standard deviation of imposed force time history of the bridge due to passage of rigid and flexible vehicle
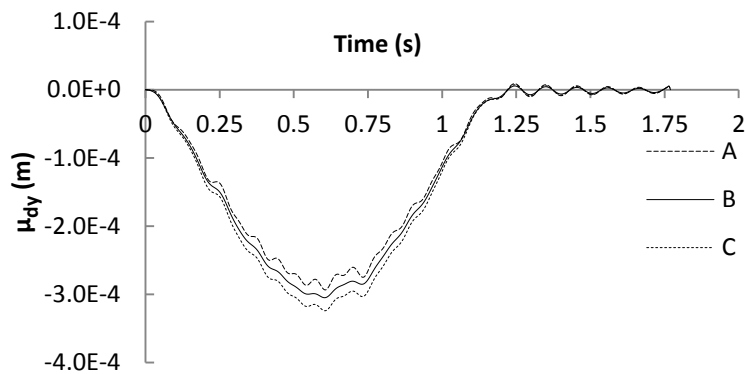

Fig. 17 Mean of bridge mid-span displacement due to different eccentricity of vehicle path (e_x), (A) e_x=0.5 m, (B) e_x =1 m, (C) e_x =1.5 m
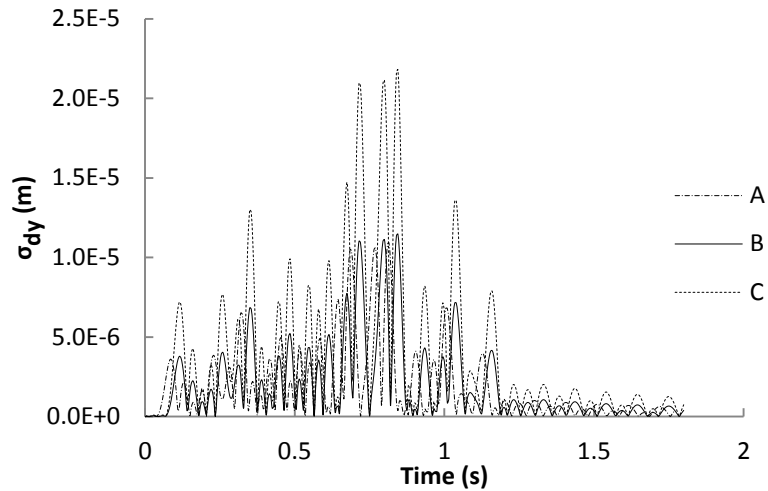
Fig. 18 Standard deviation of bridge mid-span displacement due to different eccentricity of vehicle path
(e_x), (A) e_x=0.5 m, (B) e_x =1 m, (C) e_x =1.5 m

3.5 Dynamic Amplification Factor (DAF)

Considering any response variable Y as random process, the maximum dynamic response can be written as

$$Y_{dynamic} = \left| \mu_Y(x_k,t_k) + \sigma_Y(x_k,t_k) \right| \tag{35}$$

where $Y_{dynamic}$ denotes the maximum response due to fluctuating load imposed on bridge due to vibratory motion of the vehicle excited by road unevenness.

Thus, Dynamic Amplification Factor (DAF) in this study is defined as

$$DAF = \frac{Y_{static} + Y_{dynamic}}{Y_{static}} \tag{36}$$

where Y_{static} refers to the response of the bridge at the mid span location for adverse position of static wheel loads.

3.5.1 Effect of Bridge Torsional rigidity on Dynamic Amplification Factor (DAF)

The effect of torsional rigidity of bridge has been studied by obtaining DAF for different ratios of torsional rigidity (G_bJ_b) to flexural rigidity (E_bI_b) of bridge with various values of vehicle flexural rigidity (E_vI_v) and presented in Fig. 19. The results reveal that Dynamic Amplification Factor decreases by an amount of 23% to 34% when the ratio of torsional rigidity to flexural rigidity of bridge increases from 0.002 to 0.01. This indicates that torsionally stiffer bridge produces less dynamic amplification of static live load response.
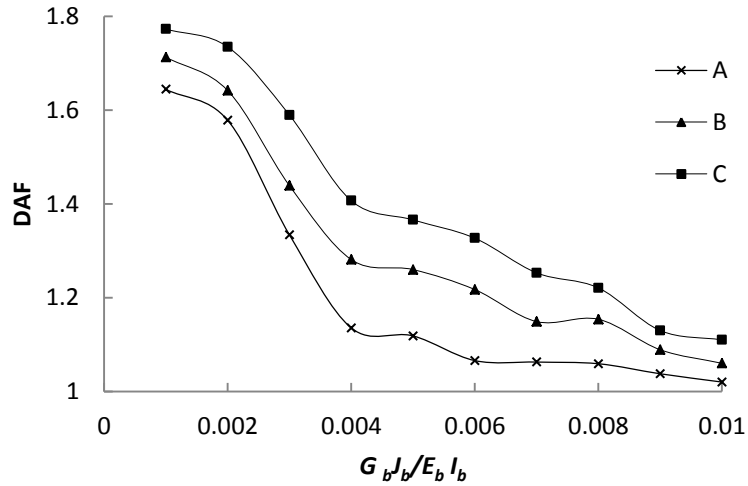
Fig. 19 Dynamic amplification factor (DAF) with the ratio of Bridge Torsional Rigidity to Flexural Rigidity ($G_b J_{b/} E_b I_b$) obtained from different vehicle flexural rigidity. (A) $E_v I_v$=5.3×10^6 N-m², (B) $E_v I_v$=6.4×10^7 N-m², (C) $E_v I_v$=8.2×10^{10} N-m²

3.5.2 Effect of vehicle axle spacing and approach slab settlement on DAF

Since dynamic amplification factor depends on several variables, we choose to represent it by surface plot rather than a two dimensional plot. The effect of vehicle axle spacing as well as approach slab settlement on the dynamic amplification factor (DAF) has been shown in Fig. 20.

Result shows that without any approach slab settlement DAF decreases with increase in vehicle axle spacing. This is expected as the increase of axle spacing causes bending modes to be more active than the rigid body modes.
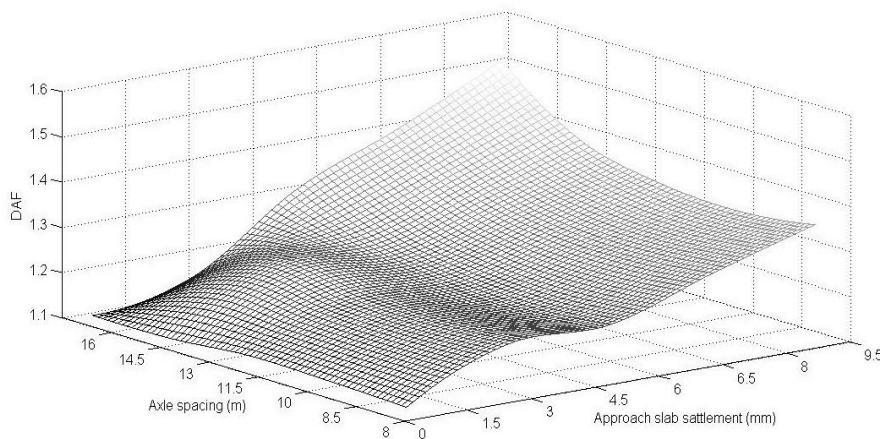

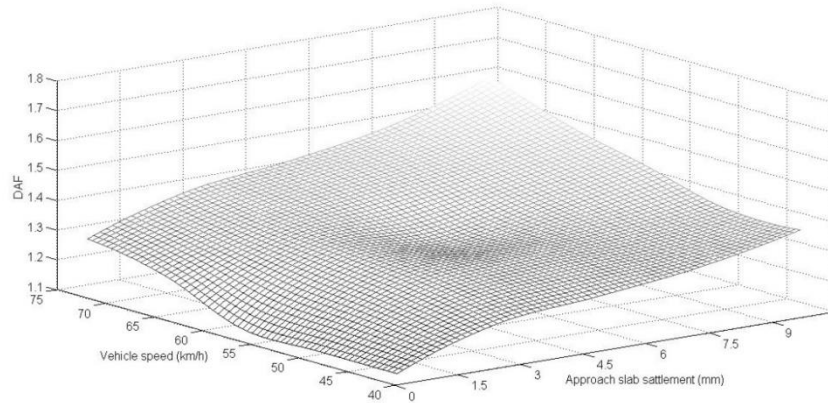Fig. 20 DAF for different axle spacing and approach slab settlement

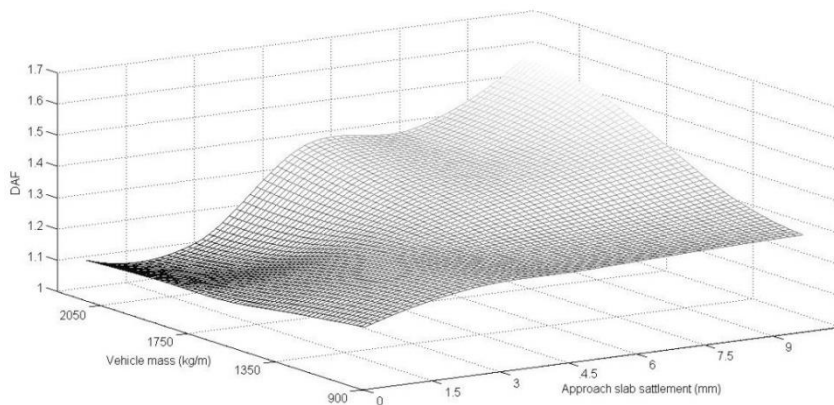Fig. 21 DAF for different vehicle speed and approach slab settlement

Fig. 22 DAF for different vehicle mass and approach slab settlement

3.5.3 Effect of vehicle speed and approach slab settlement on DAF

Combined effect of vehicle speed and approach slab settlement has been studied. Speed of the vehicle is most important factors that can cause increased dynamic amplification factor and rapid degradation of the bridge. Bridge dynamic amplification factor for 12 m vehicle axle spacing has been found by increasing approach slab settlement from zero to 9 mm with change in vehicle speed. Fig. 21 shows that larger approach slab settlement causes significant amount of transient dynamic load which produce increased deflection that becomes pronounced at higher vehicle speed.

3.5.4 Effect of vehicle mass and approach slab settlement on DAF

The present study is intended to reveal the contribution of distributed vehicle mass on the bridge response in presence of approach slab settlement. The effect of vehicle mass as well as approach slab settlement on the dynamic amplification factor (DAF) is shown in Fig. 22. It has been found that up to certain settlement of approach slab, DAF decreases with increasing vehicle

mass. Hwang and Nowak (1991) observed the same effect on DAF of bridge for a rigid model of vehicle. This may be attributed to the reason that increase of vehicle weight increases maxiumum static deflection, which in turn causes the reduction of the non dimensional DAF. However, when approach slab settlement increases from 3 mm to 9 mm, DAF is found to increase by an amount of 3.14% to 13.29% even though the static response increases with increasing weight. Result shows that when vehicle moves on a smooth deck surface, increase in its mass has not much significant effect on the bridge response, but even small and sudden difference of road profile at the bridge entry can cause considerable amount of transient response, that calls for the proper inspection and maintenance of the bridge approach and expansion joints.

3.5.5 Effect of vehicle mass and speed on DAF

The effect of vehicle mass as well as speed with the presence of approach slab settlement on the dynamic amplification factor (DAF) has been shown in Fig. 23. Individual effect on earlier classical studies has shown that effect of increasing mass has reducing effect on DAF. However, a surface plot shown in Fig. 23 shows that combined effect has an increasing trend. As mentioned in the earlier section, Hwang and Nowak (1991) argued that reduction of dynamic amplification factor with increasing vehicle weight is due to increase of static deflection. However, the coupled dynamic interaction may also be the cause of increased inertia force in addition to suspension force imposed by moving mass at greater velocity, which increases dynamic component of the response.

3.5.6 Effect of bridge surface roughness and speed

Fig. 24 shows the variation of DAF when simultaneous effect of speed and surface roughness has been considered. The surface roughness and speed of the vehicle are two most crucial factors that can cause increased dynamic amplification factor and rapid degradation of the bridge. It may be due to the fact that high speed movement of vehicle over a rough surface increases dynamic force.
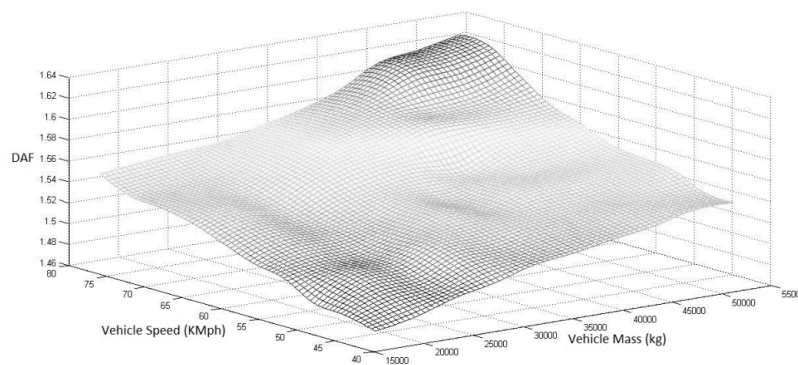

Fig. 23 Dynamic amplification factor with change in vehicle speed and vehicle mass
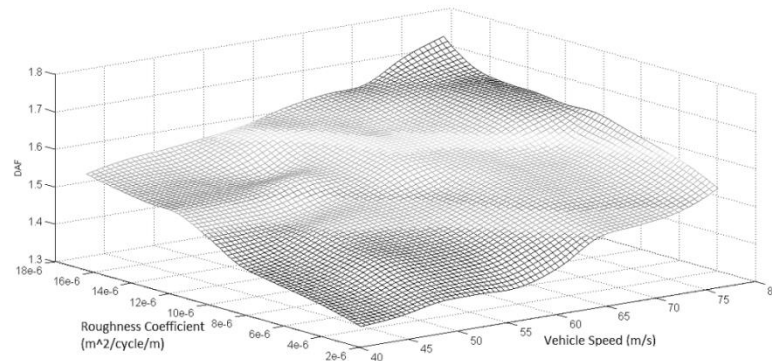
Fig. 24 Dynamic amplification factor with vehicle speed and bridge surface roughness coefficient

4. Conclusions

In the present study, coupled vehicle bridge interaction problem has been investigated considering eccentrically moving flexible vehicle. Non-homogeneity of bridge deck profile has been assumed in the formulation of the problem when a zero mean Gaussian process is superimposed over deterministic mean profiles. Response samples are generated from numerical integration and statistics are obtained. Individual and combined effects of several bridge vehicle parameters have been considered to find out the response statistics. The increased effect of vehicle speed has been found more significant in changing the frequency of imposed oscillation rather than noticeable increase in response peaks. Combined effect of increasing vehicle weight and speed has been found to increase the dynamic amplification factor. The study reveals that flexibility of long vehicle is an important consideration in obtaining bridge response and due to change in load carrying vehicle configuration, it is now imperative to address this issue in bridge design codes. Presence of approach slab settlement causes bridge dynamic response to increase when vehicle moves at higher velocity. Torsion of the bridge is activated by eccentric movement of vehicle and dynamic amplification factor is largely dependent on the ratio of torsional rigidity to flexural rigidity of bridge cross section.

Reference

Bathe, K.J. and Wilson, E.L. (1987), *Numerical methods in finite element analysis,* Prentice Hall of India Pvt. Ltd, New Delhi, India.
Biggs J.M. (1964), *Introduction to structural dynamics*, McGraw-Hill Book Co., Inc., New York, N.Y.
Brady, S. P., O'Brien, E. J. and Znidaric, A. (2006), "Effect of vehicle velocity on the dynamic amplification of a vehicle crossing a simply supported bridge", *J. Bridge Eng. - ASCE*, **11**(2), 241-249.
Chang, D and Lee, H (1994), "Impact factors for single span girder bridges", *J. Struct. Eng. - ASCE*, **120**(3), 704-715
Chen, S.R. and Cai, C.S. (2004), "Accident assessment of vehicles on long span bridges in windy environments", *J. Wind Eng. Ind. Aerod.*, **92**(12), 991-1024.
Coussy, O, Said, M. and Hoove, J.P.V. (1989), "The influence of random surface irregularities on the

dynamic response of bridges under suspended moving loads", *J. Sound Vib.*, **130**(2), 313-320

Esmailzadeh, E and Jalili, N (2003), "Vehicle-passenger-structure interaction of uniform bridges traversed by moving vehicles", *J. Sound Vib.*, **260**(4), 611-635.

Fryba, L (1968), *Vibration of solids and structures under moving loads,* Noordhoff, International Publishing, Groningen, the Netherlands.

Fryba, L. (1996), *Dynamics of Railway Bridges,* Thomas Telford, Prague*,*

Green, M.F. and Cebon, D. (1997), "Dynamic interaction between heavy vehicles and highway bridges", *Comput. Struct.*, **62**(2), 253-264

Harris, N.K., Obrien, E.J. and Gonalez, A. (2007), "Reduction of bridge dynamic amplification through adjustment of vehicle suspension damping", *J. Sound Vib.*, **302**(3), 471-485.

Hodges, D.H. and Pierce, G.A. (2002), *Introduction to Structural Dynamics and Aero-elasticity*, Cambridge Aerospace Series*.*

Huang, D. Z. and Wang, T.L. (1992), "Impact analysis of cable stayed bridges", *Comput. Struct.*, **43**(5), 897-908.

Huang, D., Wang, T.L. and Shahawy, M. (1992), "Impact analysis of continuous multigirder bridges due to moving vehicles", *J. Struct. Eng. - ASCE*, **118**(12), 3427-3443.

Hwang, E.S and Nowak, S.A. (1991), "Simulation of dynamic load for bridges", *J. Struct. Eng. - ASCE*, **117**(5), 1413-1434.

Ichikawa, M., Miyakawa, M. and Matsuda, A. (2000), "Vibration analysis of the continuous beam subjected to moving mass", *J. Sound Vib.*, **230**(3), 493-506.

Inman, D. J. (2001), *Engineering vibration*, Prentice Hall of India Pvt. Ltd, New Delhi, India.

ISO 8606 (1995), Mechanical vibration-Road surface profiles-reporting measured data.

Kozar, I. and Malic, N.T. (2013), "Spectral method in realistic modeling of bridges under moving vehicles", *Eng. Struct.*, **50**, 149-157

Law, S.S. and Zhu, X.Q. (2005), "Bridge dynamic response due to road surface roughness and effect of braking", *J. Sound Vib.*, **282**(3-5), 805-830.

Law, S.S. and Zhu, X.Q. (2005), "Bridge dynamic response due to road surface roughness and braking of vehicle", *J. Sound Vib.*, **282** (3-5), 805-830.

Lou, P. (2005), "A vehicle-track-bridge interaction element considering vehicle's pitching effect", *Finite Elem. Anal. Des.*, **41**, 397-427.

Nasrellah, H.A. and Monahar C.S. (2010), "A particle filtering approach for structural system identification in vehicle-structure interaction problems", *J. Sound Vib.*, **329**, 1289-1309.

Nigam, N.C. (1983), Introduction to random vibration, MIT Press, Cambridge

Mallic, T.N. and Kozar, I. (2012), "Vehicle strip element in the analysis of stiffened plate under realistic moving load", *Proceedings of the Institution of Mechanical Engineers*, Part-K, 226, 374-384.

Shinozuka, M. (1971), "Simulation of multivariate and multidimensional random process", *J. Acoust. Soc. Am.*, **49**, 357-367

Wang, T. L. (1992), "Dynamic response of multi girder bridge", *J. Struct. Eng. - ASCE*, **118**(8)**,** 2222-2238.

Wang, T.L., Shahawy, M. and Huang, D.Z. (1993), "Dynamic response of highway trucks due to road surface roughness", *Comput. Struct.*, **49**(6), 1055-1067.

Wang, W.J., Lu, Z.R. and Liu, J.K. (2012), "Time-frequency analysis of a coupled bridge-vehicle system with breathing cracks", *Interact. Multiscale Mech.*, **5**(3), 169-185

Wedig, W.V. (2012), "Digital simulation of road-vehicle system", *Probabilist. Eng. Mech.*, **27** 82-87

Wen, R.K. (1960), "Dynamic response of beams Traversed by Two Axle loads", *J. Eng.Mech .- ASCE*, **86**(5), 91-112.

Wu, S.Q. and Law, S.S. (2012), "Evaluating the response statistics of an uncertain bridge-vehicle system", *Mech. Syst. Signal Pr.*, **27**, 576-589.

Yang, Y.B., Yau, J.D. and Wu, Y.S. (2004), *Vehicle Bridge Interaction Dynamics with application to high speed railways*, World Scientific Publishing Co. Pte. Ltd.

Yadav, D. and Upadhyay, H.C. (1993), "Heave-Pitch-Roll dynamics of a vehicle with a variable velocity over a non-homogeneous profile flexible track", *J. Sound Vib.*, **164**, 337-348.

Yau, J.D. and Yang, Y.B. (2004), "A wideband MTMD system reducing the dynamic response of continuous truss bridges to moving train loads", *Eng. Struct.*, **261**, 795-1807.

Yang, Y.B., Li, Y.C. and Chang, K.C. (2012), "Effect of road surface roughness on the response of a moving vehicle for identification of bridge frequencies", *Interact. Multiscale Mech.*, **5**(4), 347-368

Zhang, Y., Cai, C.S. and Shi, X.M. (2006), "Vehicle induced dynamic performance of FRP versus concrete slab bridge", *J. Bridge Eng. - ASCE*, **11**(4), 410-419.